JOURNAL OF APPLIED POLYMER SCIENCE VOL. 20, 2893–2903 (1976)

A Theory for the Impact Behavior of Rate-Dependent Padding Materials

R. R. COUSINS, *National Physical Laboratory, Teddington, Middlesex TW11 OLW, England*

Synopsis

A continuum theory is used to describe the rate-dependent behavior of padding materials and is applied to predict the impact behavior of these materials when struck by flat or spherical impactors. Numerical results are given to show the effect of varying the material and geometric parameters. Some implications of the theory to practical situations are discussed.

INTRODUCTION

This paper establishes a basis for relating simple laboratory experiments on padding materials to impact applications. Particular cases of flat platens and spherical impactors are considered in detail, since they are representative of geometries involved in many applications.

Although the mechanical behavior of many materials is independent of the rate at which they are compressed, many polymeric foams used in padding applications do exhibit a dependence on strain rate. This rate dependence may be due to various factors. If the bulk material is in the transition region between its glassy and rubbery state, its properties may be strongly rate dependent.[1] In the rubbery and glassy states, the properties are much less rate dependent. Variations in the amount of rate dependence are discussed in the next section. Rate dependence may be caused by the structure of the foam. Air passing through small pores in the material will cause rate-dependent pneumatic damping.[2] Compression of gases in closed cells, as well as rupture of the cell walls, may also contribute to rate dependence.[3,4]

A continuum theory is used in the next section to model the material behavior, and it is assumed that the material response to a compressive stress is dependent on strain and rate of strain only, an assumption that has been successfully applied[5,6] to impact situations in the prediction of velocity profiles. As can be seen in those papers, velocity is not sensitive to the particular constitutive representation of the material, though the deceleration during an impact is. In this paper, a basis for predicting the deceleration as well as velocity and displacement is presented. If the theory given here is experimentally validated, it will be possible to reduce the experimental testing required in a given application and to use calculation instead. It has been shown[7] in a series of tests on polyurethane foam that cross-sectional shape and area of the foam specimen do not affect stress values, and at corresponding strains

they are not affected by foam thickness. These results give confidence in the one-dimensional theory used in the next section.

This theory can be applied directly to impacts involving flat objects, and the load on flat platens is determined in a separate section. Such geometry is of wide application in the packaging field, as it includes the protection of box-shaped goods and the padding of any flat surface. The other typical geometry considered is that of a spherical indenter striking a flat pad. This is an idealization of a corner hitting some padding, but is relevant to other applications in other fields. The one-dimensional theory previously used is adapted to give the load on a spherical indenter. It is possible to use the theory in a similar way for other simple shapes such as a cylinder, but only results for a sphere and a flat platen are presented here. In impacts, the rate of strain varies from a high initial value to zero, so that in analyzing the impact behavior of a rate-dependent material, account must be taken of the changing properties of the material during the impact. In the section on impact prediction, impact behavior is analyzed for the two geometries considered, and numerical results are presented in graphic form and discussed in the following section.

The theory used in this paper is relatively unsophisticated, and it fails to account for all aspects of an impact. Its limitations and the errors thereby introduced are discussed in the section on material characteristics. It is argued, however, that the theory is capable of giving quantitative predictions of behavior during impact. The material behavior is described in terms of three parameters, though in many cases one or two of these may be zero. It is tacitly assumed that the parameters are experimentally determined from constant rate tests, but such tests may not always be realizable. In this case, the parameters can be found from a suitable combination of impact tests with spherical and flat impactors. A final section summarizes the main conclusions.

MATERIAL CHARACTERIZATION

For the compression of a rectangular block of material by a flat platen, we assume a one-dimensional behavior. We also assume that the stress depends only on strain and rate of strain, so that we may write

$$\sigma = F(\epsilon,\dot{\epsilon}) \tag{1}$$

where σ is the stress, ϵ is the strain, and $\dot{\epsilon}$ is the strain rate. Experimental work[5,6] suggests that this dependence alone is sufficient to characterize energy-absorbing materials in impact applications. Such work also indicates that dependence on strain and strain rate is separable, so that eq. (1) may be written in the form

$$\sigma = f(\epsilon)g(\dot{\epsilon}) \tag{2}$$

It is further shown[5] that a power law representation of the rate dependence fits the data well, and for a wide class of padding materials, the constitutive equation takes the form

$$\sigma = K(1-\epsilon)^{-n}\dot{\epsilon}^{r} \tag{3}$$

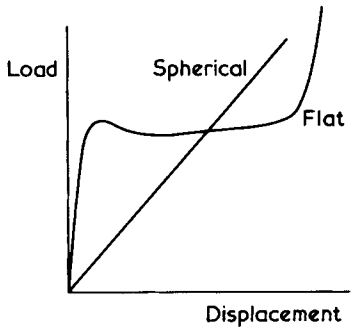

Fig. 1. Experimental curves of load/displacement in a constant rate test.[8]

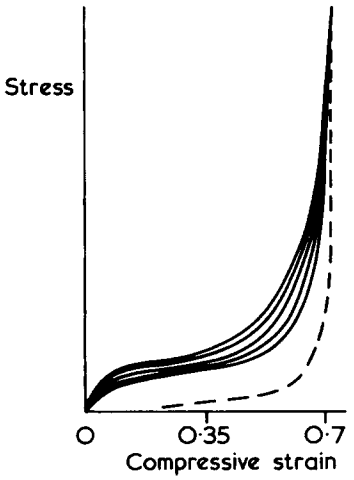

Fig. 2. Stress–strain behavior of SBR-coated urethane foam in constant rate tests[5] (velocities 33.3, 16.7, 8.3, 3.3, and 0.83 mm/s in descending order). Unloading, at all rates, given by the broken line.

where K, n, and r are constants. The indexes are typically in the ranges $0 \leqslant r \leqslant 0.3$, $0 \leqslant n \leqslant 4$. Examples of such materials exhibit the behavior shown in Figures 1 and 2. Equation (3) does not model the initial region (typically, strains less than 10%) in which the load builds up from zero to the plateau level. At high compressive strains (typically greater than 70%), the material density is considerably increased, and the load builds up rapidly. This increase is ignored in eq. (3) for $n = 0$. However, the model is good for intermediate strains which are of great practical interest. Errors in the low-strain region are usually unimportant; indeed, for spherical indenters, the difference between theory and experiment is negligible since the area of contact is small for low strains.

The use of single parameter r to model the rate dependence is valid only for a limited range of strain rates, though this range may cover several decades. In an impact, the velocity will vary from its initial value to zero, and eq. (3) predicts zero load at zero velocity for $r \neq 0$. A static loading test on the material would show that this is not true. We expect that the rate dependence would take the form of Figure 3,[5] and it is clear that static or low rate

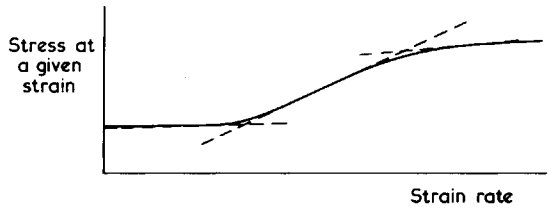

Fig. 3. Illustration of the dependence of stress on strain rate for a urethane foam[5] (logarithmic scales).

data will prove a poor guide to behavior at higher rates, a result confirmed experimentally.[7] Different values of r for the three regions in Figure 3 have been used,[5] indicated by the broken lines, though in a given impact situation only one value of r was used, that appropriate to the initial strain rate. Within the attainable experimental accuracy and the consistency of foam materials, a single parameter r is adequate to model the rate dependence, choosing the value appropriate to the steepest part of Figure 3. There are obvious dangers in extrapolating to higher or lower rates, but these are minimized in practice, as the rate in an impact soon falls. For low rates, eq. (3) underestimates the load, but the predicted peak load during the impact will not be affected. The theory also neglects any rebound. Again, the peak load is correctly predicted, and providing the rebound is slow enough to cause no further damaging impacts, it can be ignored. It is worth commenting that the comparison of impact data with calculation[1] is based on curves of velocity against strain. However, velocity is much less sensitive to a particular constitutive representation than the load, and the good correlation obtained[5] does not necessarily imply good prediction of the load profile.

LOAD ON FLAT AND SPHERICAL INDENTERS

The load on a flat indenter is readily calculated from eq. (3); providing any edge effects may be neglected, the load is

$$L = AK(1 - \epsilon)^{-n}\dot{\epsilon}^{r} \tag{4}$$

where A is the area of contact. An exact theory for a spherical indenter would need to be three-dimensional, but a modified version of the one-dimensional theory already outlined has proved to give good agreement with experiment. In this theory, the specimen is divided into thin cylindrical shells concentric with the line of travel of the center of the sphere. Each shell is of uniform height, though different shells have different heights. Each shell is assumed to deform in a one-dimensional manner according to eq. (3). The load on the sphere due to the deformation of one shell is calculated, and the total load on the sphere is obtained by integration over the region of contact.

With the notation of Figure 4, a cylindrical shell whose inner and outer walls subtend angles of 2θ and $2\theta + 2\delta\theta$ at the center of the sphere has a projected area on the base of the specimen of

$$\delta A = 2\pi R \sin\theta \cdot R\delta\theta \cdot \cos\theta \tag{5}$$

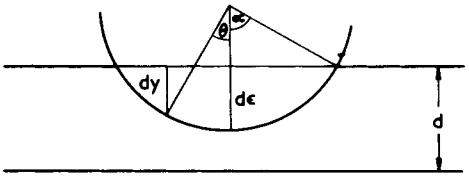

Fig. 4. Indentation of a sphere into material. Elevation through a diametrical plane.

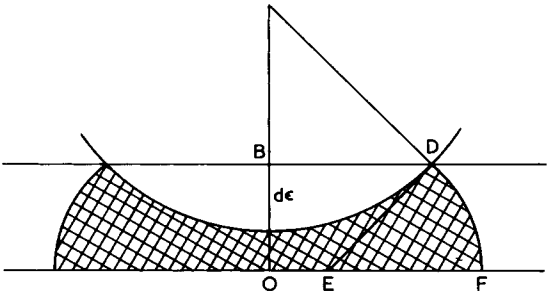

Fig. 5. Indentation of a sphere. Geometric construction to determine the stressed region.

where R is the radius of the sphere. Assuming that the shell is compressed according to one-dimensional theory, the stress is

$$\sigma = \sigma(y,\dot{y}) \tag{6}$$

Let the maximum strain be ϵ and the thickness of the material be h, so that

$$\cos\theta = 1 - h(\epsilon - y)/R \tag{7}$$

The load on the sphere due to the compression of a single shell is $\sigma\delta A$, and so the total load is

$$L = 2\pi R^2 \int_0^{\alpha} \sigma \sin\theta \cdot \cos\theta d\theta \tag{8}$$

where

$$\cos\alpha = 1 - h\epsilon/R \tag{9}$$

provided $h\epsilon \leqslant R$. The integration to determine L should only be made over the area of sphere in contact with the padding material. For $h\epsilon > R$, the upper limit in eq. (8) becomes $\pi/2$. The expression for the load can be rewritten in the form

$$L = 2\pi h^2 \int_0^{\epsilon} \sigma(y,\dot{\epsilon})(y - \epsilon + R/h)dy \tag{10}$$

with suitable modification to the lower limit when $h\epsilon > R$.

Loads calculated from eq. (10) are consistently too high, since we assume that only material directly beneath the contact area is compressed. We should expect, however, that the stressed region would be similar to the shaded area in Figure 5. This is only a simple approximation to the stressed area. Material near the circle of contact will be sheared, and no account is taken of this. The constitutive equation, however, is only approximate; and since padding materials show considerable variation in properties from sample to

sample, a more accurate and complicated approach is inappropriate. In any vertical diametrical plane through the sphere, the stress will be zero at D and at some point F on the bottom of the material, and there will be a line of zero stress joining them. The simplest form of such a curve is an arc of circle cutting the sphere and the lower face of the material normally. With the notation of Figure 5, we obtain

$$\left.\begin{aligned} \mathrm{BD} &= (2Rh\epsilon - h^2\epsilon^2)^{1/2} \\ \mathrm{OF} &= (2Rh\epsilon - h^2\epsilon^2 + h^2\epsilon)(2Rh\epsilon - h^2\epsilon^2)^{-1/2} \end{aligned}\right\} \tag{11}$$

for $h\epsilon \leqslant R$. According to the theory discussed earlier, the load on the material is supported by an area of $\pi \mathrm{BD}^2$, while the modified theory suggests that the load is supported over an area of $\pi \mathrm{OF}^2$. The stress levels previously obtained were too high, and we now divide them by a factor of $\pi \mathrm{DF}^2/\pi \mathrm{BD}^2$, so that the corrected load on a sphere is

$$L = 2\pi h^2 \left(1 + \frac{1}{2R/h - \epsilon}\right)^{-2} \int_0^{\epsilon} \sigma(y,\dot{\epsilon})(y - \epsilon + R/h)dy \tag{12}$$

We shall work throughout assuming $\epsilon < R$, though appropriate modification can be made for deeper penetrations. Adjustments can be made, too, for small specimens for which the stressed region extends to the edge of the material.

IMPACT PREDICTION

Flat Indenters

Let us consider a flat indenter of mass M per unit area striking some material of thickness h at an impact velocity of $h\eta$, where η is the initial strain rate. From eq. (4), the equation of motion is

$$Mh\ddot{\epsilon} = -K(1 - \epsilon)^{-n}\dot{\epsilon}^r \tag{13}$$

which, on writing $\ddot{\epsilon} = \dot{\epsilon}d\dot{\epsilon}/d\epsilon$ and integrating, gives

$$\dot{\epsilon} = \eta(1 - a\lambda(\epsilon))^{1/(2-r)} \tag{14}$$

where a is the nondimensional parameter

$$a = (2 - r)K/Mh\eta^{2-r} \tag{15}$$

and

$$\left.\begin{aligned} \lambda(\epsilon) &= -\log(1 - \epsilon) && \text{for } n = 1 \\ &= \{(1 - \epsilon)^{1-n} - 1\}/(n - 1) && \text{otherwise} \end{aligned}\right\} \tag{16}$$

This indenter will be brought to rest when $\dot{\epsilon} = 0$, which, from eq. (14), implies

$$\left.\begin{aligned} \epsilon &= 1 - \exp(-1/a) && \text{for } n = 1 \\ &= 1 - \left(1 + \frac{n-1}{a}\right)^{1/(1-n)} && \text{otherwise} \end{aligned}\right\} \tag{17}$$

TABLE I
Maximum Deceleration During the Impact of a Flat Indenter

r	$n = 0$	$n = 1$	$n \neq 0,1$
0	$a/2$	$\frac{a}{2}e^{1/a}$	$\frac{a}{2}\left[1+\frac{n-1}{a}\right]^{\frac{n}{n-1}}$
$\neq 0$	$\frac{a}{2-r}$	$\frac{a}{2-r}\left[\frac{ar}{2-r}\right]^{\frac{r}{2-r}}\exp\left[\frac{1}{a}-\frac{r}{2-r}\right]$	$\frac{a}{2-r}\left\{\frac{(2-r)n(n-1+a)}{a(2n-r)}\right\}^{\frac{n}{n-1}}\left\{\frac{r(n-1+a)}{2n-r}\right\}^{\frac{r}{2-r}}$

We note the important special case of $n = 0$. Then, $\lambda = \epsilon$, and the body comes to rest when $\epsilon = a^{-1}$. If $a < 1$, however, the indenter will not be stopped. In practice, the theory with $n = 0$ will break down for $\epsilon > 0.7$, say, and the load will increase rapidly at high strains to stop the indenter before ϵ reaches 1.

By integrating eq. (14), we obtain the nondimensional time

$$\eta t = \int_0^{\epsilon} (1 - a\lambda(x))^{-1/(2-r)} dx \tag{18}$$

and substituting eq. (14) into eq. (13) the nondimensional deceleration is

$$\eta^{-2}|\ddot{\epsilon}| = a(2-r)^{-1}\eta^r(1-\epsilon)^{-n}\,(1 - a\lambda(\epsilon))^{r/(2-r)} \tag{19}$$

From eq. (19), we can calculate the maximum deceleration during the impact; the results are given in Table I.

Spherical Indenters

The load on a spherical indenter was derived in the previous section. Writing

$$\rho = R/h,\ b = \frac{8\pi K h \rho^2 (2-r)}{M(1+2\rho)^2\eta^{2-r}} \tag{20}$$

where M is the mass of the sphere and R is its radius, we obtain from eq. (12) the equation of motion of the sphere:

$$\ddot{\epsilon} = \frac{b\eta^{2-r}}{2-r}\,\dot{\epsilon}^r\,(1-\epsilon/2\rho)^2\,\{1-\epsilon/(2\rho+1)\}^{-2}\,\mu(\epsilon) \tag{21}$$

where

$$\left.\begin{aligned}
\mu(\epsilon) &= \epsilon(\rho - \epsilon/2) \quad \text{for } n = 0 \\
&= -\epsilon - (1-\epsilon+\rho)\log(1-\epsilon) \quad \text{for } n = 1 \\
&= \epsilon(1-\epsilon+\rho)/(1-\epsilon) + \log(1-\epsilon) \quad \text{for } n = 2 \\
&= (1-\epsilon+\rho)\{(1-\epsilon)^{1-n} - 1\}/(n-1) - \{(1-\epsilon)^{2-n} - 1\}/(n-2) \quad \text{otherwise}
\end{aligned}\right\} \tag{22}$$

On integrating (21), we obtain

$$\dot{\epsilon} = \eta\left\{1 - b\int_0^{\epsilon} \mu(x)(1-x/2\rho)^2\{1-x/(2\rho+1)\}^{-2}dx\right\}^{1/(2-r)} \tag{23}$$

which may be substituted in eq. (21) to give $\ddot{\epsilon}$ as a function of ϵ.

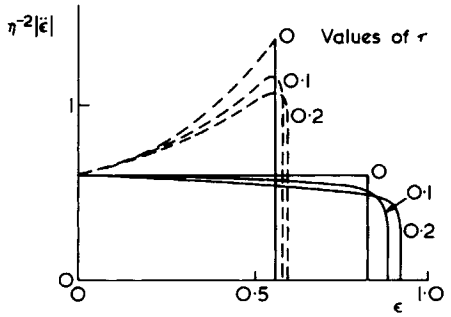

Fig. 6. Deceleration of a flat indenter for varying rate dependence with $n = 0$ (solid curves) and $n = 1$ (broken curves); $a = 1.2, 1.14, 1.08$ for $r = 0, 0.1, 0.2$, respectively.

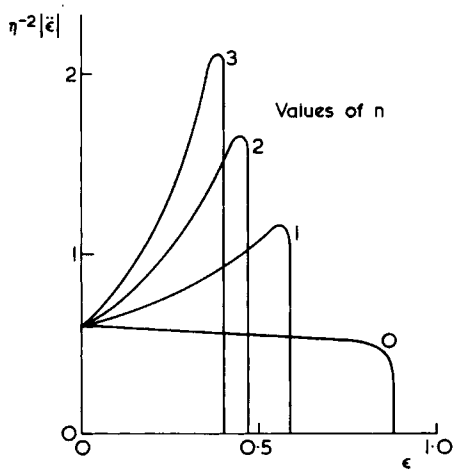

Fig. 7. Deceleration of a flat indenter hitting materials with different values of n; $a = 1.14$, $r = 0.1$.

NUMERICAL RESULTS

Some numerical results obtained from the theory of the previous section are given in Figures 6–11. The first three figures indicate the loads on a flat indenter, given in nondimensional form. In Figure 6, we see that a rate-dependent material causes a lower load than the equivalent rate-independent material (for $n > 0$). The parameter a was chosen to give the same initial deceleration, so that we are comparing materials with the same response at the initial rate of strain. From Figure 7, it is clear that a material with a flat stress–strain response in constant rate tests ($n = 0$) is more desirable, since it gives a lower peak load. However, a greater thickness of material is required. Different impact speeds are compared in Figure 8. Values of a were chosen so that the initial decelerations reflect changes in η only, and the strain deceleration is plotted rather than the nondimensional deceleration of earlier figures. The rise in peak loading with increasing impact speed is due to two factors, higher velocities and greater penetration. The first cause does not apply to a rate-independent material, and the second does not affect the loading for materials with $n = 0$.

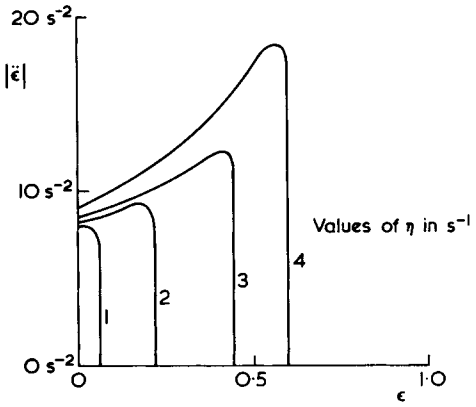

Fig. 8. Deceleration of a flat indenter striking padding at different rates; $n = 1$, $r = 0.1$; $a = 15.0, 4.03, 1.71, 1.08$ for $\eta = 1, 2, 3, 4\ s^{-1}$, respectively.

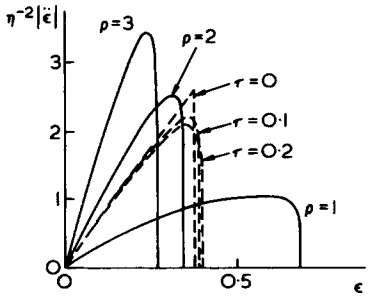

Fig. 9. Deceleration of a spherical indenter during impact for different values of r (broken curves, $\rho = 3$) and ρ (solid curves, $r = 0.1$); $n = 0$; $b = 5.0, 4.75, 4.5$ for $r = 0, 0.1, 0.2$, respectively (broken curves); $b = 6.667, 9.6, 11.02$ for $\rho = 1, 2, 3$, respectively (solid curves).

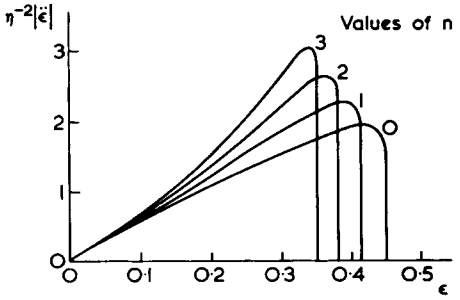

Fig. 10. Deceleration of a spherical indenter hitting materials with different values of n; $r = 0.1$, $b = 3.6$, $\rho = 3$.

Results for spherical indenters are shown in Figures 9–11. In Figure 9, the effects of varying r and ρ are compared, and parameter b is chosen to reflect changes in these parameters alone. We note, as for flat indenters, that the peak loading decreases with increasing rate dependence. A smaller sphere penetrates further into the material than a larger one, but at a lower deceleration. Alternatively, the figure may be interpreted to show, for a given sphere, that a thicker pad of material will lead to lower loads. Materials with differ-

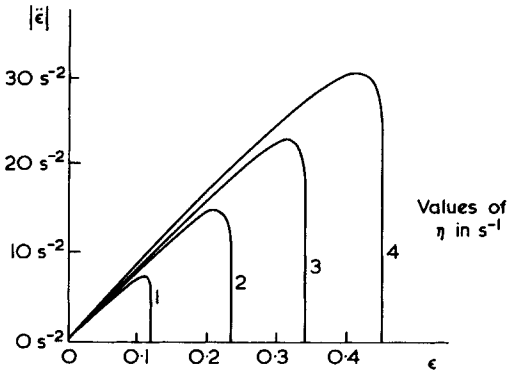

Fig. 11. Deceleration of a spherical indenter at different impact speeds; $n = 0$, $r = 0.1$, $\rho = 3$; $b = 50.0, 13.4, 6.2, 3.6$ for $\eta = 1, 2, 3, 4\ s^{-1}$, respectively.

ent values of n are compared in Figure 10; the peak load increases with n, while the penetration decreases. The effect of different impact speeds is shown in Figure 11. Parameter b is chosen to reflect changes in η only. Higher impact speeds require deeper penetration into the material to absorb the impact energy, and this leads to higher loads. The effect of higher peak loads with increasing η would be still greater for materials with $n > 0$.

CONCLUSIONS

A theory has been given to describe the impact behavior of padding materials. The rate dependence of such materials can be adequately modeled by a power law model, and two other parameters have proved sufficient to describe the strain dependence. The relevant quantities required in assessing the suitability of a material for a given impact application are the maximum deceleration of the impacting object, the depth of penetration into the padding, and, possibly, the duration of the impact. A simple formula gives those quantities directly for a flat impactor. For a spherical indenter, however, the full time history of the impact must be computed to give these quantities.

For a flat impactor, a rate-dependent material has advantages over a rate-independent material. The peak loading is slightly less, but, more importantly, for a lower impact speed, the load is less. For a spherical indenter, the peak loading is again slightly less for a rate-dependent material, but the reduction for lower impact speeds is insignificant compared with the reduction in load resulting from a smaller area of contact at the lower speeds. It should be noted that when the compressive strain exceeds about 70%, the load rises rapidly; and if such strains are anticipated, the backing structure can be designed to yield at an appropriate stress level to reduce any further compression of the foam. An example from the packaging industry is a packing case consisting of a wooden box with an interior foam lining. An article inside will be cushioned by the foam, but when the load reaches a sufficiently high value, the wooden casing will bend and absorb some of the energy.

It is not envisaged that the work reported here will eliminate all impact testing of padding materials, but it should enable the choice of materials to be narrowed before impact tests are carried out and the number of these tests to be reduced.

The author would like to thank Mrs. A. Woolf for undertaking the computation involved in this paper.

References

1. J. D. Ferry, *Viscoelastic Properties of Polymers,* 2nd ed., Wiley, New York, 1961, Chap. 2, p. 42.
2. A. N. Gent, and K. C. Rusch *Rubber Chem. Technol.,* **39,** 389 (1966).
3. D. R. Otis, *Thermal Damping in Gas-Filled Composite Materials During Impact,* University of Wisconsin, Madison, 1968.
4. D. R. Otis, *Impact Loading of a Closed-Cell, Foamed Elastometer,* University of Wisconsin, Madison, 1968.
5. D. M. Schwaber and E. A. Meinecke, *J. Appl. Polym. Sci.,* **15,** 2381 (1971).
6. E. A. Meinecke, D. M. Schwaber, and R. R. Chiang, *J. Elastoplastics,* **3,** 19 (1971).
7. P. N. Rao and K. E. Hofer, *J. Mat. JMLSA,* **6,** 704 (1971).
8. W. M. Lee, *Proc. Fifth Int. Conf. on Rheology, Univ. of Tokyo Press,* **3,** 83 (1970).

Received September 15, 1975